

# Differential inelastic electron scattering cross sections from experimental reflection electron-energy-loss spectra: Application to background removal in electron spectroscopy

S. Tougaard and I. Chorkendorff

*Fysisk Institut, Odense Universitet, DK-5230 Odense M, Denmark*

(Received 4 September 1986; revised manuscript received 15 December 1986)

The possibility of extracting absolute inelastic electron scattering cross sections  $K(T)$  (differential in energy loss  $T$  and path length) for solids from experimental electron spectra is studied. Assuming homogeneous scattering properties for the solid, a formula is found, which allows a direct determination of  $[\lambda L / (\lambda + L)]K(T)$  from a measured reflected electron-energy-loss spectrum (REELS) resulting from a monoenergetic beam of electrons incident on the surface of the solid. Here  $\lambda$  is the inelastic electron mean free path and  $L \simeq 2\lambda_1$  where  $\lambda_1$  is the transport mean free path for elastic electron scattering. The formula is applied to experimental REELS spectra of aluminum. The resulting cross sections are discussed in relation to a theoretical calculation based on dielectric-response theory. The determined cross sections are applied to remove the inelastic background signal from  $\text{Mg-}K\alpha$  ( $h\nu \simeq 1254$  eV) and synchrotron-radiation-excited ( $h\nu \simeq 250$  eV) photoelectron spectra of aluminum. The resulting primary excitation spectra are discussed in relation to the results of existing procedures.

## I. INTRODUCTION

The elastic and inelastic electron scattering properties of solids have been studied extensively in the past.<sup>1-3</sup> These investigations have concentrated on high-energy electrons and today only very limited quantitative information is available on the differential inelastic scattering cross sections for electrons in the low-energy range ( $\leq 10$  keV).

Previously, theoretical calculations based on dielectric response theory<sup>4,5</sup> have been performed.<sup>5-8</sup> In this approach experimental, optical, or high-energy electron transmission data are used to obtain the dielectric-response function  $\epsilon(0, \omega)$  in the limit of zero momentum transfer. However, a problem arises because theoretical extrapolations have to be made to describe  $\epsilon(k, \omega)$  for nonzero momentum transfer  $k$ .

In the present paper we study the possibility of extracting quantitative information on the electron scattering properties of a solid through the analysis of experimental electron spectra. It is clear that the energy spectrum of backscattered electrons resulting from bombarding the solid surface with a monoenergetic beam of electrons will contain information both on elastic and on inelastic scattering properties of the solid. The technique, known as reflection electron-energy-loss spectroscopy (REELS) has been used extensively in the past to obtain qualitative information on the electronic properties of solids.<sup>1,9,10</sup>

In order to extract *quantitative* information on cross sections from REELS, a model for the transport of electrons in the solid is essential. Based on recent progress in such models,<sup>11-14</sup> we derive a formula here [Eq. (11)] which under certain conditions directly allows the determination of  $[\lambda L / (\lambda + L)]K(T)$  from an experimental REELS spectrum  $j_i(E)$ . Here  $K(T)$  is the differential cross section for electron-energy loss  $T$ ,  $\lambda$  is the mean free path for inelastic electron scattering, and  $L$  is related to the elastic scattering properties of the solid (see Sec. II).

The application of the formula is demonstrated for experimental REELS spectra of aluminum. Aluminum was chosen because here one clearly observes distinguished structure corresponding to multiple excitations of plasmons. As a result, the origin of different features in  $K(T)$  are clearly identified. This provides a convenient basis for a test of the validity and the limitations of the formula. Being a free-electron-like metal, aluminum also allows us to compare the result to theoretical cross sections evaluated from dielectric-response theory.<sup>4,7</sup>

Detailed knowledge of differential inelastic scattering properties are of great importance for the surface-sensitive Auger-electron spectroscopy (AES) and x-ray-photoelectron spectroscopy (XPS). These spectroscopies operate through an analysis of electrons excited to kinetic energies in the range studied here. Quantitative application of AES and XPS must rely heavily on knowledge of the scattering properties of the solid.<sup>8,11-15</sup>

As an example, we apply the present cross sections to remove the inelastic background signal from the  $\text{Mg } K\alpha$  and the synchrotron-radiation-excited photoelectron spectrum  $j_x(E)$  of aluminum by the use of an existing formula<sup>11</sup> [Eq. (14)]. Since the prefactor on the integrals in Eqs. (11) and (14) are approximately identical, this can be performed without the use of adjustable parameters. Finally, the relation to existing procedures for background removal in electron spectroscopy is discussed.

## II. THEORY

### A. Inelastic scattering cross sections from REELS

Let the solid surface be bombarded with a monoenergetic flux  $F(E) = \delta(E - E_0)$  of electrons. We assume that the solid has homogeneous scattering properties to all depths of relevance here. This is a good approximation at high kinetic energies, but will break down at low energies

(see Sec. IV A). Further, we assume that the scattering properties of the solid are independent of energy within the energy range of a REELS spectrum. This is well fulfilled in the energy range  $E_0 - E \ll E_0$  of interest here. Then the flux of backreflected electrons have an energy and angular distribution given by<sup>11,13</sup>

$$J_l(E, \Omega) = \int dR Q(E_0, \Omega_0, x=0; R, \Omega) G(E_0, R; E), \quad (1)$$

where  $Q(E_0, \Omega_0, x; R, \Omega) dR d^2\Omega$  is the probability for an electron with initial energy  $E_0$  and direction  $\Omega_0$  to pass a plane at depth  $x$  in direction  $(\Omega, d^2\Omega)$  after having traveled a path length  $R$  in the solid.  $G(E_0, R; E)$  is the probability that an electron with initial energy  $E_0$  has energy  $E$  after having traveled the path length  $R$  in the solid.

Recently, Tofterup showed<sup>13</sup> that the path-length distribution is approximately given by

$$Q(R) = A(\eta_0, \eta) \lambda_1^{-1} e^{-R/L}, \quad (2)$$

where the attenuation length  $L \simeq 2\lambda_1$ . Here,  $\lambda_1$  is the transport mean free path for elastic electron scattering.  $A(\eta_0, \eta)$  is a function of the directional cosines of the incident ( $\eta_0$ ) and exit ( $\eta$ ) angles of the electron. We use the Landau expression<sup>16</sup> for the energy distribution as a function of  $R$ :

$$G(E_0, R; E) = \frac{1}{2\pi} \int_{-\infty}^{\infty} ds \exp[is(E_0 - E) - R\Sigma(s)], \quad (3)$$

where

$$\Sigma(s) = \int_0^{\infty} dT K(T) (1 - e^{-isT}). \quad (4)$$

Here,  $K(T)$  is the probability that an electron shall lose energy  $T$  per unit energy loss and per unit path length traveled in the solid. After inserting Eq. (3) in Eq. (1) and performing the integration over  $R$ , we find

$$J_l(E, \Omega) = \frac{A(\eta_0, \eta)}{\lambda_1} \int ds \frac{e^{is(E_0 - E)}}{\Sigma(s) + 1/L}. \quad (5)$$

Now, in analogy with previous work,<sup>11,12</sup> we Fourier-transform Eq. (5), first with respect to  $E$  then with respect to  $s$ , and find

$$\frac{\lambda L}{\lambda + L} K(E_0 - E_i) = \left[ j_l(E_i) - \sum_{m=1}^{i-1} \frac{\lambda L}{\lambda + L} K(E_0 - E_{i-m}) j_l(E_m) \Delta E \right] / [j_l(E_0) \Delta E], \quad (12)$$

where  $j_l(E_0) \Delta E = A_p$  is the integrated intensity in the elastic peak.

If the REELS spectrum is only measured in the  $E < E_0^-$  energy range, the recursion formulas [Eqs. (11) and (12)] are still valid. Thus, in this case we get, from Eq. (12),

$$\begin{aligned} & \frac{\lambda L}{\lambda + L} K(E_0 - E_i) \\ &= \frac{1}{c} \left[ j_l(E_i) - \sum_{m=1}^{i-1} \frac{\lambda L}{\lambda + L} K(E_0 - E_{i-m}) j_l(E_m) \Delta E \right], \end{aligned} \quad (13)$$

$$\begin{aligned} \frac{A(\eta_0, \eta)}{\lambda_1} \delta(E_0 - E) &= \frac{\lambda + L}{\lambda L} J_l(E, \Omega) \\ &\quad - \int dE' K(E' - E) J_l(E', \Omega). \end{aligned} \quad (6)$$

When only relative intensities within a measured spectrum are considered, we define

$$j_l(E) \equiv J_l(E, \Omega) \frac{\lambda + L}{\lambda L} \frac{\lambda_1}{A(\eta_0, \eta)}, \quad (7)$$

and get

$$\delta(E_0 - E) = j_l(E) - \frac{\lambda L}{\lambda + L} \int_E^{\infty} dE' K(E' - E) j_l(E'). \quad (8)$$

Since  $j_l(E) = 0$  for  $E > E_0^+$  and since

$$\int_{E_0^-}^{E_0^+} K(E' - E) j_l(E') dE' \simeq K(E_0 - E) \int_{E_0^-}^{E_0^+} j_l(E') dE', \quad (9)$$

we have

$$\begin{aligned} \delta(E_0 - E) &= j_l(E) - \frac{\lambda L}{\lambda + L} \int_E^{E_0^-} K(E' - E) j_l(E') dE' \\ &\quad - \frac{\lambda L}{\lambda + L} K(E_0 - E) A_p, \end{aligned} \quad (10)$$

where

$$A_p = \int_{E_0^-}^{E_0^+} j_l(E') dE'$$

is the elastic peak area.

For  $E \leq E_0^-$  we then find a recursion formula for the determination of  $[\lambda L / (\lambda + L)] K(T)$ ,

$$\begin{aligned} & \frac{\lambda L}{\lambda + L} K(E_0 - E) \\ &= \frac{j_l(E) - \int_E^{E_0^-} \frac{\lambda L}{\lambda + L} K(E' - E) j_l(E') dE'}{\int_{E_0^-}^{E_0^+} j_l(E') dE'}. \end{aligned} \quad (11)$$

Dividing the REELS spectrum into channels  $E_i$  of width  $\Delta E$ , we may rewrite Eq. (11):

where  $c = j_l(E_0) \Delta E$  is now an unknown quantity which may be used as a scaling parameter. The application of Eq. (13) is discussed in detail in a separate paper.<sup>17</sup>

## B. Inelastic background removal in XPS

In x-ray-excited photoelectron spectroscopy of homogeneous solids, primary electrons are excited homogeneously to essentially infinite depth. Let  $F_x(E_0)$  denote the primary excitation spectrum at the point of excitation in the solid and let  $j_x(E)$  denote the measured energy spectrum of emitted electrons. Then,<sup>11,14</sup>

$$F_x(E) = j_x(E) \frac{\lambda L_x}{\lambda + L_x} \int_E^\infty dE' K(E' - E) j_x(E'), \quad (14)$$

where  $L_x \simeq 5\lambda_1$ . Knowledge of  $[\lambda L / (\lambda + L)]K(T)$  from an experimental REELS spectrum [Eq. (11) or (12)] can now directly be used in Eq. (14) and the primary photon-excited energy spectrum  $F_x(E)$  be determined. Note that the prefactor on the integral is different in Eq. (14) compared to Eq. (11). However, since in typical cases<sup>18</sup>  $\lambda_1 > \lambda$ , the prefactor is expected to be only slightly modified (see also Sec. IV A). Therefore, if values of  $L$  and  $L_x$  are not known, the prefactor may be used as a fitting parameter (see also the example in Sec. IV B, where the prefactor is assumed unchanged).

A procedure frequently used in background subtraction in electron spectroscopy<sup>19-21</sup> is strongly connected with the above. It may be derived in the following way. The XPS spectrum from a homogeneous sample is<sup>11,14</sup>

$$J_x(E, \Omega) = A_1(\eta) \int dE' F(E') \int dR e^{-R/L_x} G(E', R; E), \quad (15)$$

where  $A_1(\eta)$  is a function of the directional cosine of the emitted electrons. The REELS spectrum from the same sample is from Eqs. (1) and (2):

$$J_l(E_0 - E, \Omega) = \frac{A(\eta_0, \eta)}{\lambda_1} \int dR e^{-R/L} G(E_0, R; E). \quad (16)$$

Within the approximation that  $L_x \simeq L$  and  $E' \simeq E_0$ , we therefore have

$$J_x(E, \Omega) = \frac{A_1(\eta)}{A(\eta_0, \eta)} \lambda_1 \int dE_0 F_x(E_0) J_l(E_0 - E, \Omega). \quad (17)$$

Now we insert  $j_l(E, \Omega)$  from Eq. (6) rearrange and find, for the relative intensity in  $F_x(E)$ ,

$$F_x(E) = j_x(E) - c_1 \int_E^\infty dE' F_x(E') j_l(E' - E). \quad (18)$$

The method, recently described by Burrell and Armstrong,<sup>21</sup> now consists of sequentially removing the background signal from the measured spectrum. If the intensity on the low-energy side of the spectrum is not zero after the first iteration, the value of  $c_1$  is changed. In this way a value of  $c_1$  is found iteratively. This procedure is effectively identical to the use of Eq. (13), i.e., without measuring the REELS spectrum in the elastic peak. Then the unknown quantity  $c = j_l(E_0) \Delta E$  in Eq. (13) is used as an adjustable parameter. The value is determined by the requirement that after the deconvolution formula (14) is applied, the XPS intensity must be zero on the low-energy side of the spectrum (see Ref. 17).

### C. Inelastic background removal in AES

In x-ray-excited AES, primary electrons are excited to essentially infinite depth. Therefore Eq. (14) also applies here. In electron- or ion-bombardment-stimulated AES one faces two complications. Thus the backreflected primary electrons and the secondary electrons must initially be removed in order to isolate the contribution to the spectrum from the Auger electrons.<sup>22</sup> The second prob-

lem here is that due to the slowing down of the bombarding particles and to the effect of backscattered electrons, the excitation is not homogeneous to infinite depths. To the extent that the intensity in the primary spectrum varies exponentially with distance to the solid surface, a deconvolution formula similar to Eq. (14) is valid.<sup>12</sup> The only change lies in the prefactor on the integral, which may then be used as a fitting parameter. Note, however, that the in-depth intensity of Auger-electron emitters depends critically on both the exciting beam energy and on the excitation by backscattered electrons.<sup>23,24</sup>

## III. EXPERIMENTAL DETAILS

The experiments were performed in an ultrahigh-vacuum (UHV) chamber with a base pressure below  $10^{-10}$  Torr. A thick layer of high-purity aluminum (99.999%) was evaporated onto a stainless-steel substrate. Since here we are studying electron transport in a homogeneous medium, it is highly important to ensure that the Al film thickness is sufficient to be considered a homogeneous semi-infinite medium.

Evaporation was done step by step. It was noticed that after the Fe lines had disappeared from the XPS spectrum, the background signal in the (100–300) eV energy range below the Al 2s peak did still change significantly with subsequent evaporations of Al. Evaporation was continued until the intensity down to 300 eV from the Al 2s peak did not change with subsequent evaporations of aluminum.

The reflected electron-energy-loss spectra were measured under an angle of 25° between the electron gun and the entrance slit of the 150° hemispherical electron-energy analyzer. The XPS spectra were measured in the same setup and were excited by Mg K $\alpha$  radiation. The spectra were averaged over three scans and taken with the analyzer (VG-CLAM 100) in the constant-pass energy mode. All spectra were corrected for the analyzer transmission function, which in this mode is proportional to  $E^{-0.45}$ , where  $E$  is the kinetic energy of the detected electrons.<sup>25</sup> A photoelectron spectrum excited by synchrotron radiation ( $h\nu \simeq 250$  eV) was taken at HASYLAB in Hamburg. The Al sample used was cleaned by Ar-ion bombardment and annealed to remove implanted Ar atoms. This spectrum was also corrected for the analyzer transmission function.

## IV. EXPERIMENTAL RESULTS AND DISCUSSION

### A. Electron scattering cross sections

Figure 1 shows experimental REELS spectra  $j_l(E)$  of aluminum at selected primary electron energies  $E_0$ . Structure corresponding to multiple-surface and bulk-plasmon excitations are clearly seen. As expected, the strength of the first surface relative to the first bulk plasmon decreases as the primary energy is increased.

Now Eq. (12) was applied to these spectra and  $[\lambda L / (\lambda + L)]K(T)$  was determined *without the use of any*

*fitting parameters.* The result in Fig. 2 essentially shows a two-peak structure. The peak energies  $T_S \approx 10$  eV and  $T_B \approx 15$  eV correspond to surface- and bulk-plasmon excitations, respectively. Slight negative values of  $K(T)$  are observed in the energy region  $T \approx T_S + T_B$ , while a small

peak occurs at  $T \approx 2 \cdot T_B$ . For higher energy loss,  $K(T)$  rapidly approaches zero. Although double bulk-plasmon excitation in a single-scattering event is possible, the major contribution to the peak at  $T \approx 2T_B$ , as well as the unphysical negative cross sections at  $T \approx T_S + T_B$ , are primarily ascribed to differences in the theoretical and the experimental situations. Thus, in Sec. II A, the sample was treated as a homogeneous medium. The assumption made was that as the primary electron travels in the solid, the probability  $K(T)$  for energy loss  $T$  per unit path

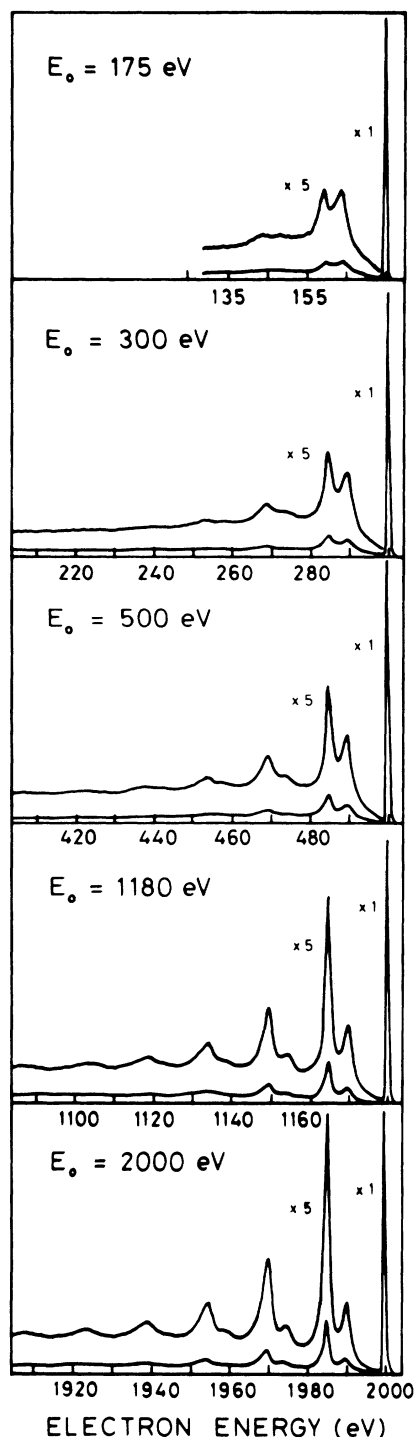


FIG. 1. Experimental REELS spectra  $j_l(E)$  of aluminum for various primary electron energies  $E_0$ . The structure corresponds to multiple surface- and bulk-plasmon excitations.

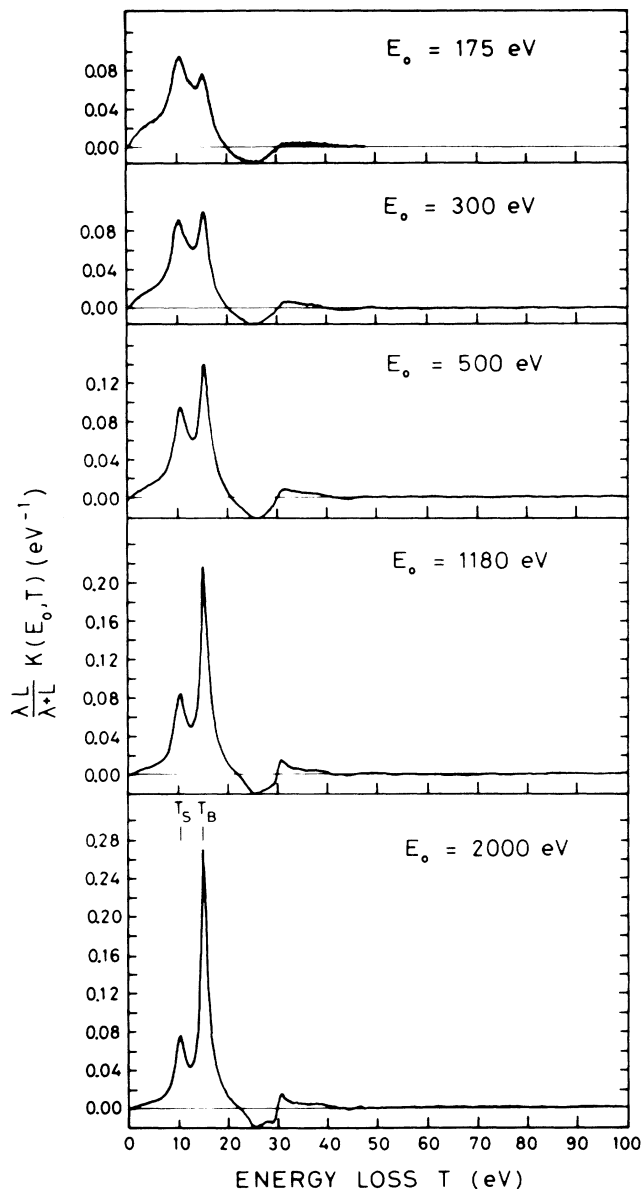


FIG. 2. Differential inelastic electron scattering cross sections  $[\lambda L / (\lambda + L)] K(E_0, T)$  determined numerically from Eq. (12) with  $j_l(E)$  taken from the experimental data in Fig. 1. The peak energies  $T_S \approx 10$  eV and  $T_B \approx 15$  eV correspond to surface- and bulk-plasmon excitations, respectively. The unphysical negative cross sections at  $T \approx T_S + T_B$  are ascribed to differences between the theoretical and the experimental situations. See text.

length and per unit energy loss is a constant function of  $T$ , independent of the actual depth underneath the sample surface. It is, however, clear that the probability of exciting a surface plasmon decreases and the probability of exciting a bulk plasmon increases with depth. Therefore, the relative intensities in the various multiple surface- and

bulk-plasmon excitation peaks will be slightly different in the real sample, compared to the idealistic sample with homogeneous scattering properties treated in Sec. II A.

For comparison with the curves in Fig. 2 we have evaluated theoretical cross sections for inelastic scattering in aluminum. We use the Lindhard expression<sup>4</sup>

$$K(E_0, \hbar\omega) = \frac{1}{\pi E_0 a} \int_{k^-}^{k^+} \frac{dk}{k} \text{Im} \left[ -\frac{1}{\epsilon(k, \omega)} \right], \quad (19)$$

where

$$k_{\pm} = (2m/\hbar^2)^{1/2} (\sqrt{E} \pm \sqrt{E - \hbar\omega}),$$

$a_0$  is the Bohr radius, and  $\epsilon(k, \omega)$  is the complex dielectric function of the solid. To model  $\text{Im}[-1/\epsilon(k, \omega)]$  we follow previous work<sup>7,12,26</sup> and use a free-electron gas including damping to describe collective excitations, while the contribution from single-electron excitations are evaluated from the Lindhard dielectric function. With the notation of Ref. 7, the plasmon parameter values determined from the best fit to the experimental data in Fig. 2 are  $\gamma = 0.8$  eV and  $X_p = 15.0$  eV. These values deviate from the values ( $\gamma = 0.25$  eV and  $X_p = 14.9$  eV) found in Ref. 27. This is due to the much improved experimental resolution of the electron spectrometer used here. Values of the inelastic mean free path  $\lambda$  were taken from Ref. 7.

Figure 3 shows the resulting theoretical  $\lambda K(T)$  functions at selected primary electron energies  $E_0$ . The absolute ordinate scale is the same, while the abscissa scale is changed in comparison with Fig. 2. The surface-plasmon peak is, of course, nonexistent in the theoretical cross sections (Fig. 3). Therefore, especially at low  $E_0$ , the bulk-plasmon peak height is smaller in Fig. 2 compared to Fig. 3. As  $E_0$  is increased, the cross section, as determined from the experimental REELS spectra and Eq. (12) (Fig. 2), gradually approaches the theoretical cross sections. Note that in Fig. 3 we have assumed  $L \gg \lambda$ . Finite values of  $L$  would decrease the values in Fig. 3 and bring them into closer agreement with Fig. 2. The effect is, however, small since  $L \simeq 2\lambda_1$  and  $\lambda_1 > \lambda$  (see Table I).

Information on elastic electron scattering is also con-

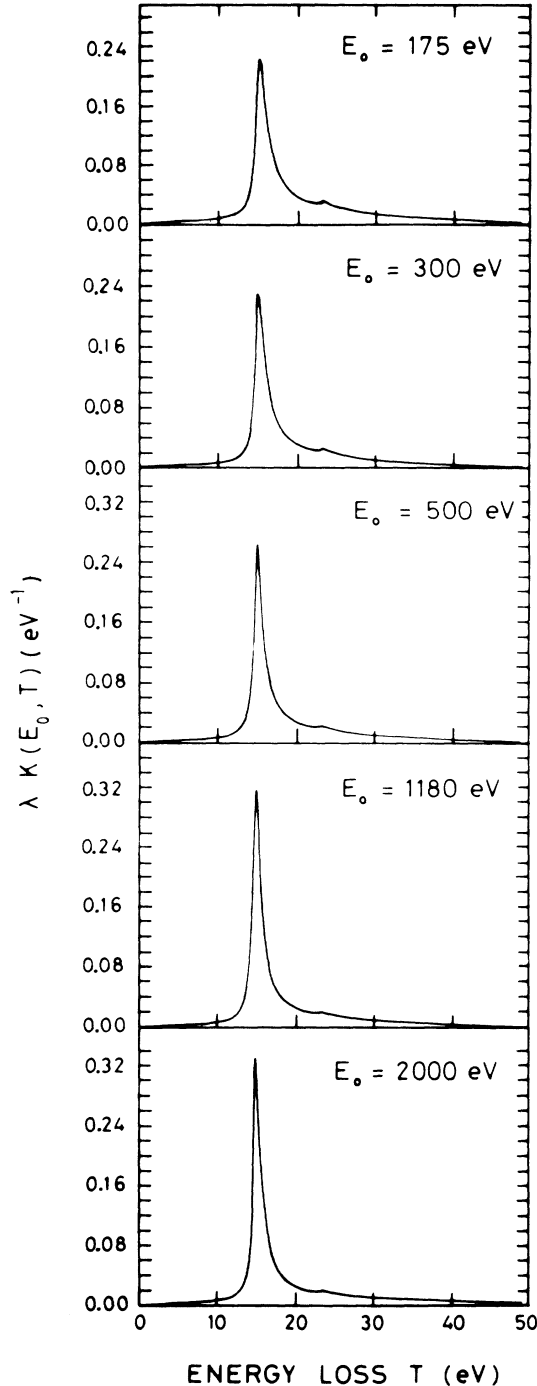


FIG. 3. Theoretical differential inelastic electron scattering cross sections  $\lambda K(E_0, T)$  for aluminum determined numerically from Eq. (19). Note that the ordinate scale is the same, while the abscissa scale is changed in comparison with Fig. 2.

TABLE I. Values of  $[\lambda L / (\lambda + L)] \int_0^{100 \text{ eV}} K(T) dT$  as determined from the experimental curves in Fig. 2 and theoretical values of  $\lambda$  (Ref. 7) at various primary electron energies  $E_0$ .  $L$  is found by Eq. (20) and  $\lambda_1$  is taken from an atomic calculation (Ref. 18). Values of  $\lambda_1$  in parentheses are extrapolated from the data in Ref. 18.

$E_0$ (eV)	$\frac{\lambda L}{\lambda + L} \int_0^{100 \text{ eV}} K(T) dT$	$\lambda^a$ (Å)	$L$ (Å)	$\lambda_1^b$ (Å)
175	0.779	5.6	19.7	(10)
300	0.873	8.3	57.1	(20)
500	0.910	12.4	125	(50)
1180	0.940	23.5	368	180
1400	0.944	27.0	455	220
2000	0.950	36.0	684	413

<sup>a</sup>Reference 7.

<sup>b</sup>Reference 18.

tained in the REELS spectra. Thus, from the definition of  $K(T)$  and  $\lambda$ , we have

$$\frac{\lambda L}{\lambda + L} \int_0^{E_0} K(T) dT = \frac{L}{\lambda + L}. \quad (20)$$

Table I shows values of

$$\frac{\lambda L}{\lambda + L} \int_0^{100 \text{ eV}} K(T) dT$$

as determined from the curves in Fig. 2. With the  $\lambda$  values taken from Ref. 7,  $L$  can finally be found from Eq. (20). The values given in Table I for the transport mean free path for elastic electron scattering in aluminum are evaluated from an atomic calculation.<sup>18</sup> As mentioned above, a calculation based on a  $P_1$  approximation to the Boltzmann transport equation predicts  $L \simeq 2\lambda_1$ .<sup>13</sup> This is in fair agreement with the data in Table I, for which we have  $L \simeq 2\lambda_1$  for all  $E_0$ .

### B. Application to inelastic background removal in electron spectroscopy

As discussed in Secs. II B and II C, detailed knowledge of  $K(T)$  is essential for quantitative analysis of electron spectra. In this section we will apply Eq. (14) to remove the inelastic intensity contribution from the experimental XPS spectrum of aluminum. We will use two approximations to the cross section: (1)  $K(T)$  evaluated from theory, Eq. (19), and (2)  $K(T)$  determined from a REELS spectrum, Eq. (12), and will compare the resulting primary spectra  $F_x(E_0)$ .

Figure 4(a) shows the experimental Mg  $K\alpha$  excited Al XPS spectrum after subtraction of a constant background and after correcting for the analyzer transmission function (upper spectrum). The lower spectrum is the result of applying Eq. (14) to this spectrum with  $L_x \rightarrow \infty$  and with  $\lambda K(T)$  taken from the theoretical calculation at  $E_0 = 1180$  eV (Fig. 3). Here a reduction in  $\lambda$  from the theoretical value  $23.5 \text{ \AA}$  to  $20.6 \text{ \AA}$  was allowed to account partly for the finite value of  $L_x$  and partly for the uncertainty in the theoretical  $\lambda$  value. Then, on the low-energy side of the spectrum, essentially all intensity is removed in the deconvoluted spectrum. Some intensity remains in the energy region of the first bulk-plasmon energy loss of both the Al 2s and Al 2p peaks. This is expected because many-electron effects always cause a photoexcitation peak to be accompanied by electrons at lower energy.<sup>28-30</sup> The surface-plasmon peaks are, of course, not removed since the possibility of surface-plasmon excitations is not included in the model.

The lower spectrum in Fig. 4(b) results from using Eq. (14) with  $[\lambda L_x / (\lambda + L_x)] K(T)$  taken from the experimentally determined function  $[\lambda L / (\lambda + L)] K(T)$  at  $E_0 = 1180$  eV (Fig. 2). The prefactor was assumed identical (i.e.,  $L \simeq L_x$ ). Also, here, essentially all intensity on the low-energy side of the spectrum is removed *without using adjustable parameters*. In the region of the surface-plasmon loss we get negative intensities in the primary spectrum. As in Fig. 4(a), some intensity remains, as expected in the first plasmon peak.

The main difference between the primary spectra  $F_x(E)$

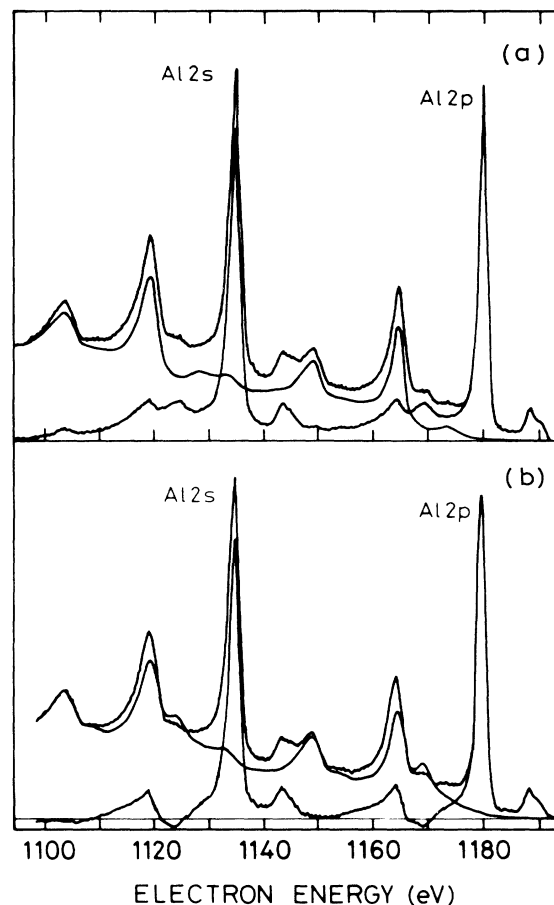


FIG. 4. Experimental Mg  $K\alpha$ -excited photoelectron spectrum of aluminum (upper curves) and the primary electron excitation spectra as determined by Eq. (14) (lower curves). The difference curves are the background signal of inelastically scattered electrons. In (a)  $[\lambda L_x / (\lambda + L_x)] K(T)$  was taken from theory (Fig. 3,  $E_0 = 1180$  eV) assuming  $L_x \rightarrow \infty$  and  $\lambda = 20.6 \text{ \AA}$  (see text). In (b)  $[\lambda L_x / (\lambda + L_x)] K(T)$  was taken from the experimentally determined  $[\lambda L / (\lambda + L)] K(T)$  (Fig. 2,  $E_0 = 1180$  eV) assuming  $L_x \simeq L$ .

in Figs. 4(a) and 4(b) resulting from the use of the two cross sections lies in the strength of the first surface relative to the first bulk-plasmon loss of the two main Al 2s and Al 2p peaks. In Fig. 4(b), the applied cross section  $K(T)$  is based on a REELS spectrum (Fig. 2). These electrons have passed the surface region twice. In the XPS spectrum the electrons have passed the surface region only once. As a result, when  $K(T)$  from Fig. 2 is applied to an XPS spectrum [by Eq. (14)] the surface-plasmon strength is overestimated. With the same arguments, we conclude that the strength of the bulk plasmon is underestimated. Therefore in Fig. 4(b) we expect to remove too much intensity in the energy region of the first surface plasmon and too little intensity around the bulk plasmon. This explains the occurrence of the unphysical negative intensities in Fig. 4(b). Using the theoretical cross sections [Fig. 4(a)], on the other hand, it is obvious that we remove too little intensity around the surface-plasmon

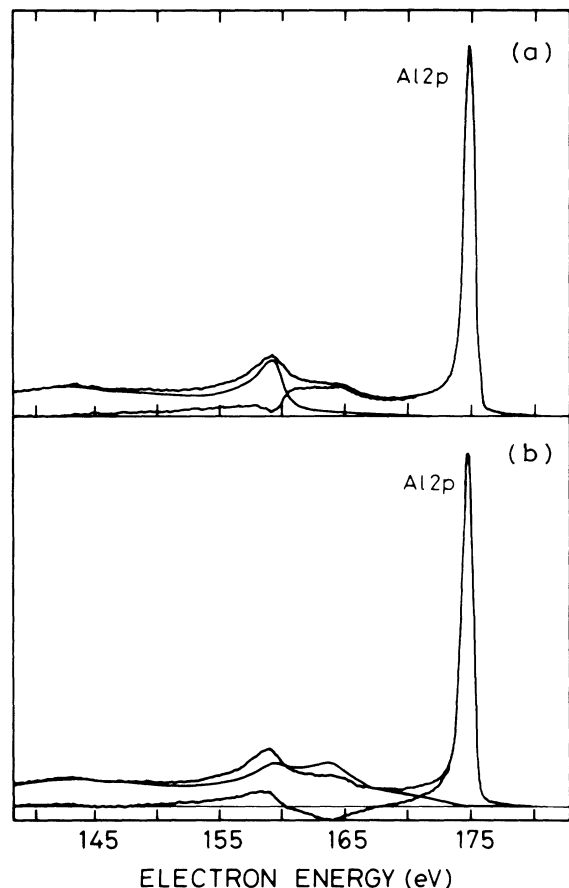


FIG. 5. Experimental synchrotron-radiation- ( $h\nu \approx 250$  eV) excited photoelectron spectrum of aluminum (upper curves) and the primary electron excitation spectra as determined by Eq. (14) (lower curves). The difference curves are the background signal of inelastically scattered electrons. In (a),  $[\lambda L_x / (\lambda + L_x)]K(T)$  was taken from theory (Fig. 3,  $E_0 = 175$  eV) assuming  $L_x \rightarrow \infty$  and  $\lambda = 3.8$  Å. In (b),  $[\lambda L_x / (\lambda + L_x)]K(T)$  was taken from the experimentally determined  $[\lambda L / (\lambda + L)]K(T)$  (Fig. 2,  $E_0 = 175$  eV) assuming  $L_x \approx L$ .

and too much around the bulk-plasmon energy loss. The true primary excitation spectrum must therefore lie somewhere between the two lower spectra in Figs. 4(a) and 4(b).

Finally, Figs. 5(a) and 5(b) show the result of a similar analysis of the synchrotron-photon-excited Al 2p spectrum. The features observed are quite similar to those discussed above. Since the kinetic energy of the electrons is considerably lower here compared to Fig. 4, the surface-plasmon loss peak plays a more prominent role. For the same reasons as in Fig. 4(a) (see above), the value of  $\lambda$  was, in Fig. 5(a), reduced from the theoretical value 5.6 Å to 3.8 Å. In Fig. 5(b) no adjustable parameters were used.

Note that the shape of the intrinsic bulk plasmon in the background-corrected spectra in Figs. 4 and 5 deviate considerably from the shape of the bulk plasmon in the REELS spectra. This may be due to the difference in the excitation mechanisms in the two cases.<sup>31</sup>

The result of the deconvolution method based on Eq. (13) or (18) will depend on the exact procedure chosen for the iterative determination of  $c$  and  $c_1$ , respectively. Since we are then entering the regime of mathematical and leaving the regime of physical modeling, this falls outside the scope of the present paper.

### C. General remarks

Two different, although strongly related, physical problems have been treated in the present paper:

(1) A new method is found for the experimental determination of differential inelastic scattering cross sections for electrons in homogeneous solids. The method consists of a simple analysis [by Eq. (11)] of a reflection electron-energy-loss spectrum resulting from bombarding the sample surface with a monoenergetic beam of electrons. The present method has, particularly for low-energy electrons, great advantages over existing methods. Thus, electron-transmission experiments have previously been successfully applied in the experimental investigation of electron cross sections.<sup>1</sup> This technique is, however, not applicable to low-energy electrons due to obvious experimental problems in producing and handling extremely thin films.

(2) It is at present clear that the greatest problem in background subtraction in electron spectroscopy is the general lack of knowledge of the differential inelastic electron scattering cross section.<sup>30,32</sup> In this paper we have therefore also discussed the possibility of using the determined cross sections in the analysis of experimental AES and XPS spectra. It is, however, clear from the observed negative intensities in Figs. 4 and 5 that this paper does not provide a final solution to the general problem of background removal in electron spectroscopy. As mentioned above, the formulas are only exact for homogeneous solids. Most real samples are inhomogeneous within the surface region and, as discussed in Sec. IV A, the cross section, even for a homogeneous sample, is expected to be depth dependent.

Alternative ways of obtaining the cross section necessary for background removal in XPS and AES from homogeneous samples have been discussed in other works.<sup>12,15,33</sup> Currently, effort is being spent in finding deconvolution formulas valid for the analysis of inhomogeneous samples.<sup>12,32</sup>

The advantage of these methods as well as of the method presented here is that they do *not* involve adjustable parameters, they do *not* rely on an iterative procedure, and they *are based on a physical model*. Therefore a discussion of possible errors in the background-corrected spectrum is possible.

### V. CONCLUSIONS

We assumed homogeneous electron scattering properties of the surface region of a solid. Then a formula was found [Eq. (11)] which allows a determination of  $[\lambda L / (\lambda + L)]K(E_0, T)$  from a measured energy-loss spectrum  $j_i(E)$  of backscattered electrons resulting from bombarding the solid surface with a monoenergetic beam of electrons of energy  $E_0$ . Here,  $K(E_0, T)$  is the probability that an electron of energy  $E_0$  shall lose energy  $T$  per unit

energy loss and per unit path length traveled in the solid,  $\lambda$  is the inelastic electron mean free path, and  $L \simeq 2\lambda_1$ , where  $\lambda_1$  is the transport mean free path for elastic electron scattering. The formula was applied to experimental loss spectra of Al and the resulting cross sections were compared to an evaluation based on dielectric response theory. Deviations primarily resulting from the breakdown of the assumption of homogeneous scattering prop-

erties of the solid to all depths were discussed. The determined cross sections were, via an existing formula [Eq. (14)], applied to remove the background of inelastically scattered electrons from Mg  $K\alpha$ - ( $h\nu \simeq 1254$  eV) and synchrotron-radiation- ( $h\nu \simeq 250$  eV) excited photoelectron spectra of aluminum. The resulting primary spectra were discussed in relation to the result of existing procedures.

- 
- <sup>1</sup>See, for example, H. Raether, *Excitations of Plasmons and Interband Transitions by Electrons*, Vol. 88 of *Springer Tracts in Modern Physics* (Springer, New York, 1980).
- <sup>2</sup>M. Inokuti, *Rev. Mod. Phys.* **43**, 297 (1971).
- <sup>3</sup>International Commission on Radiation Units and Measurements, Report No. 37 ISBN 0-913394-31-9, 1984 (unpublished).
- <sup>4</sup>J. Lindhard, K. Dan. Vidensk. Selsk. Mat.-Fys. Medd. **28**, No. 8 (1954).
- <sup>5</sup>R. H. Ritchie and A. Howie, *Philos. Mag.* **36**, 463 (1977).
- <sup>6</sup>J. C. Ashley, J. J. Cowan, R. H. Ritchie, V. E. Anderson, and J. Holzl, *Thin Solid Films* **60**, 361 (1979).
- <sup>7</sup>C. J. Tung and R. H. Ritchie, *Phys. Rev. B* **16**, 4302 (1977).
- <sup>8</sup>S. Tougaard and B. Jørgensen, *Surf. Sci.* **143**, 482 (1984).
- <sup>9</sup>R. Dorn, H. Lüth, and M. Buchel, *Phys. Rev. B* **16**, 4675 (1977).
- <sup>10</sup>F. P. Netzer and M. M. El Gomati, *Surf. Sci.* **124**, 26 (1983).
- <sup>11</sup>S. Tougaard and P. Sigmund, *Phys. Rev. B* **25**, 4452 (1982).
- <sup>12</sup>S. Tougaard, *Surf. Sci.* **139**, 208 (1984).
- <sup>13</sup>A. Tofterup, *Phys. Rev. B* **32**, 2808 (1985).
- <sup>14</sup>A. Tofterup, *Surf. Sci.* **167**, 70 (1986).
- <sup>15</sup>S. Tougaard and B. Jørgensen, *Surf. Interface Anal.* **7**, 17 (1985).
- <sup>16</sup>L. Landau, *J. Phys. (Moscow)* **8**, 201 (1944).
- <sup>17</sup>I. Chorkendorff and S. Tougaard (unpublished).
- <sup>18</sup>M. E. Riley, C. J. MacCallum, and F. Briggs, *At. Data Nucl. Data Tables* **15**, 443 (1975); **28**, 379 (1983).
- <sup>19</sup>W. M. Mularie and W. T. Peria, *Surf. Sci.* **26**, 125 (1971).
- <sup>20</sup>H. H. Madden and J. E. Houston, *J. Appl. Phys.* **47**, 3071 (1976).
- <sup>21</sup>M. C. Burrell and N. R. Armstrong, *Appl. Surf. Sci.* **17**, 53 (1983).
- <sup>22</sup>E. N. Sickafus, *Surf. Sci.* **100**, 529 (1980).
- <sup>23</sup>M. M. El Gomati and M. Prutton, *Surf. Sci.* **72**, 485 (1978).
- <sup>24</sup>S. Ichimura and R. Shimizu, *Surf. Sci.* **112**, 386 (1981).
- <sup>25</sup>M. P. Seah, *Surf. Interface Anal.* **2**, 222 (1980); VG-CLAM 100 manual, 1982.
- <sup>26</sup>P. C. Gibbons, S. E. Schnatterly, J. J. Ritsko, and J. R. Fields, *Phys. Rev. B* **13**, 2451 (1976).
- <sup>27</sup>S. Tougaard and I. Chorkendorff, *Solid State Commun.* **57**, 77 (1986).
- <sup>28</sup>G. K. Wertheim and S. Hufner, *Phys. Rev. Lett.* **35**, 53 (1975).
- <sup>29</sup>D. R. Penn, *Phys. Rev. Lett.* **40**, 568 (1978).
- <sup>30</sup>S. Tougaard, *Phys. Rev. B* **34**, 6779 (1986).
- <sup>31</sup>D. Šokčević and M. Šunjić, *Phys. Rev. B* **30**, 6965 (1984).
- <sup>32</sup>S. Tougaard, *J. Vac. Sci. Technol.* (to be published).
- <sup>33</sup>S. Tougaard, *Solid State Commun.* **61**, 547 (1987).